SPECIAL PROJECT PROGRESS REPORT

All the following mandatory information needs to be provided. The length should *reflect the complexity and duration* of the project.

Reporting year	2022
Project Title:	FLEXPART energy transport simulations and inverse modelling of atmospheric constituents
Computer Project Account:	spatvojt
Principal Investigator(s):	Martin Vojta
Affiliation:	University of Vienna – Department of Meteorology and Geophysics
Name of ECMWF scientist(s) collaborating to the project (if applicable)	…… ……
Start date of the project:	2021
Expected end date:	2023

Computer resources allocated/used for the current year and the previous one

(if applicable)

Please answer for all project resources

		Previous year		Current year	
		Allocated	Used	Allocated	Used
High Performance Computing Facility	(units)	1000000		2000000	
Data storage capacity	(Gbytes)	10000		20000	

Summary of project objectives (10 lines max)

The Lagrangian particle dispersion model FLEXPART (Stohl et al., 2005, Pisso et al., 2019) is run on ECMWF data to explore the dispersion and transport of various atmospheric constituents. The model is used with inversion techniques to enhance the knowledge about the emissions of many atmospheric compounds. This helps to get a better understanding of their impact on the Earth's climate system and air quality and to improve transport simulations of these substances. By performing domain-filling simulations the model is used to develop Lagrangian climatologies of heat and energy transport in the atmosphere and to perform case studies of extreme weather events.

Summary of problems encountered (10 lines max)

……

Summary of results

If submitted **during the first project year**, please summarise the results achieved during the period from the project start to June of the current year. A few paragraphs might be sufficient. If submitted **during the second project year**, this summary should be more detailed and cover the period from the project start. The length, at most 8 pages, should reflect the complexity of the project. Alternatively, it could be replaced by a short summary plus an existing scientific report on the project attached to this document. If submitted **during the third project year**, please summarise the results achieved during the period from July of the previous year to June of the current year. A few paragraphs might be sufficient.

1) Lagrangian re-analysis Dataset

By performing domain-filling transport model simulations with the Lagrangian particle dispersion model, as well as forward and backward simulations for particular sites, Lagrangian transport climatologies, as well as global statistics can be established. We created a Lagrangian re-analysis, based on the ERA-5 dataset from ECMWF, on a one-hourly basis. Therefore, five million particles were released at the first timestep, globally distributed and transported forward in time. These particles remain in the atmosphere over the whole time period and represent the atmospheric mass. The dataset ranges from 1979 to 2022 and consists of five million trajectories that are 42 years long.

By using this Lagrangian Reanalyses Dataset, the energy export from the Equatorial Pacific, and how it is affected by the El-Niño-Southern-Oscillation (ENSO) is detected. Therefore, only particles that have been in the Nino3.4 and Nino3 region and below 1 km were selected and followed 20 days forward in time. We then determine the mass fraction r of the transported tagged air relative to its environment, the total air, present in a volume. We further determine how different the transported tagged air is relative to the untagged environmental air in potential temperature and specific humidity. By using the Nino3.4 Index, we consider how these impacts of the transported tagged air are changing with ENSO.

Furthermore, the Lagrangian Reanalyses Dataset is used to study extreme heat wave events, for example the extreme heat wave over Western Canada in June 2021. Therefore, particles from the target region are followed backward in time, in order to identify where they are coming from and how their meteorological properties are changing along the transport. In the future, this method will be adopted to other extreme heat wave events, to gain a better overview on the role of atmospheric transport when considering such extremes.

2) A comprehensive evaluation of the use of Lagrangian particle dispersion models for inverse modelling of greenhouse gas emissions

Using the example of sulfur hexafluoride (SF_6) we investigate the use of Lagrangian Particle Dispersion Models (LPDMs) for inverse modelling of greenhouse gas (GHG) emissions and explore the limitations of this approach. We put the main focus on the impacts of baseline methods and the LPDM backward simulation

period on the a posteriori emissions determined by the inversion. We consider baseline methods that are based on a statistical selection of observations at individual measurement sites, like the REBS method (Ruckstuhl et al., 2012) or a method introduced by Stohl et al. (2009). Apart from that, we investigate a global distribution-based (GDB) approach, where global mixing ratio fields are coupled to the LPDM back-trajectories at their termination points. In this project, we used the hourly meteorological re-analysis dataset ERA5 from ECMWF for two purposes: (1) the Lagrangian particle dispersion model FLEXPART was driven with ERA5 to calculate the source-receptor relationship on which the inversion is based on, and (2) ERA5 was used to perform a global re-analysis of SF_6 for the year 2012, since global fields of SF_6 mixing ratios were needed in order to apply the global distribution-based method.

We show (Figure 1) that purely statistical baseline methods cause large systematical errors, which lead to inversion results that are highly sensitive to the LPDM backward simulation period and can generate unrealistic global total a posteriori emissions. The GDB method produces a posteriori emissions that are far less sensitive to the backward simulation period and that are consistent with recognized global total emissions.

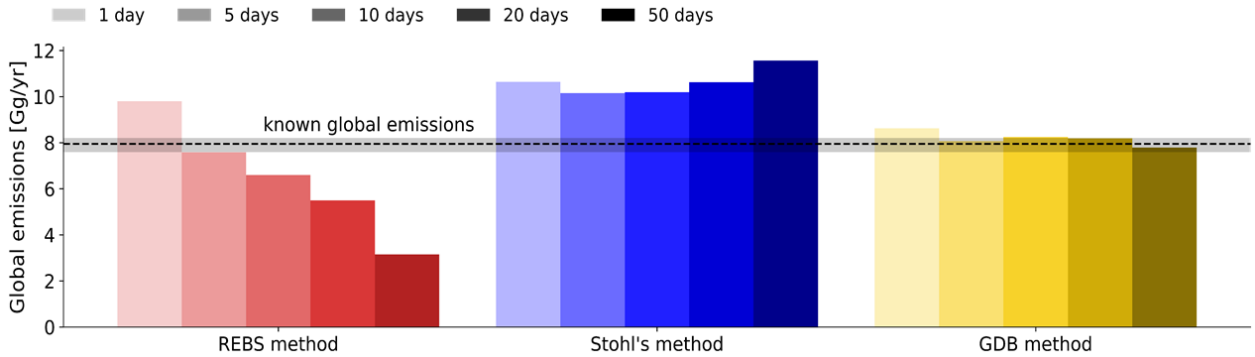

Figure 1: SF_6 global emissions derived by the inversions. Results are shown for the three applied baseline methods and for the five applied backward simulation periods between 1 and 50 days. The horizontal dashed line represents the reference value of the AGAGE 12-box model with shaded error bands.

Our results further show that longer backward simulation periods, beyond the often used 5 to 10 days, reduce the mean squared error and increase the correlation between a priori modeled and observed mixing ratios. Also, the inversion becomes less sensitive to biases in the a priori emissions and the global mixing ratio fields for longer backward simulation periods. Further, longer periods help to better constrain emissions in regions poorly covered by the global SF6 monitoring network, as shown in Figure 2 in terms of emission increments (i.e. a posteriori minus a priori emissions).

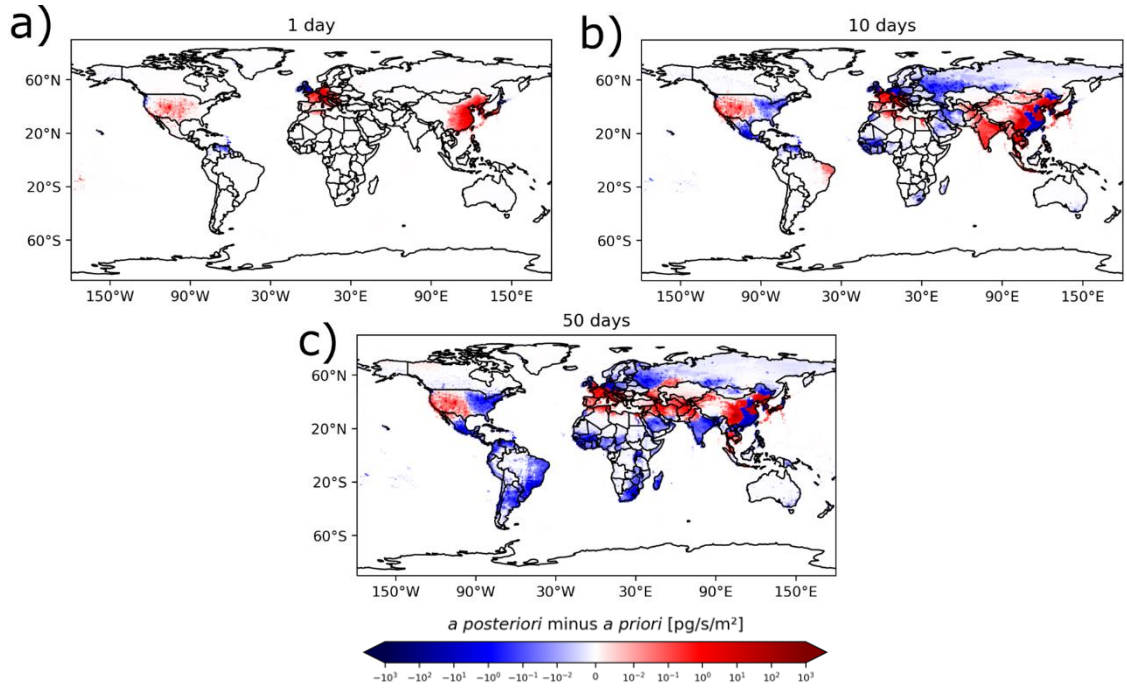

Figure 2: SF_6 emission increments calculated with the inversion by using the GDB method and a backward simulation period of a) 1 day, b) 10 days and c) 50 days

Furthermore, we find that the inclusion of existing flask measurements in the inversion helps to further close these gaps and suggest that a few additional and well placed flask sampling sites would have great value for improving global a posteriori emission fields.

3) Interpretation of ice core data

We are collaborating with scientists all over the world by helping to interpret deposition of various species found in ice core records. It is essential to understand the atmospheric pathways the deposited particles took, in order to be able to identify potential emission source regions. For this, we run global FLEXPART simulations driven by ERA5 reanalysis data at a horizontal and temporal resolution of 0.5° and 1 hour, respectively. FLEXPART is used in backward mode, releasing virtual particles and sending them backward in time from individual ice cores sites to identify potential emission source regions for each ice core site. However, FLEXPART is also used in forward mode, releasing particles from known or suspected emission sources to identify the most promising ice core sites at which most deposition might have occurred.
Figure 3 shows emission sensitivity maps derived from backward FLEXPART simulations for four different ice core sites. The plots indicate the deposition signal (in μg/m2/a) an emission of unit strength (1 kg/s) at any given grid cell would have on the respective site. In other words, the ice core locations are more sensitive to emissions from brighter (yellow/orange) regions than they are to emissions from (darker) blue/violet regions. Figure 3 (upper left) shows the emissions sensitivities for the Summit site in Greenland indicating for example that Summit is more sensitive to Northern American than Eurasia. Figure 3 (upper right) illustrates the strong isolation of Antarctic ice core sites (here: Hercules Dome), the strongest sensitivities are on the continent itself and the surrounding ocean. Only the southern tips of South America, Africa, and Australia are sampled by this ice core. Furthermore, Figure 3 (lower left and lower right) shows the emission sensitivities for an Andean site (Illimani) and Mt. Elbrus in the Caucasus. We also performed simulations for Alpine ice core sites (not shown).

Recently, we have been involved in studies investigating:

- The 20th century Thallium emissions in Western Europe as recorded in an ice core extracted at the Col du Dome site in the French Alps.
- Sources of black carbon recorded in an array of Northern mid- and high-latitude ice cores from 1850 to 2000.
- Early Andean, Spanish Colonial, and Industrial-era mining emissions recorded in several Antarctic ice cores.
- The decoupling of Canadian forest dynamics from climate following European settlement by analyzing pollen preserved in two Greenlandic ice cores.
- The consistent histories of anthropogenic Western European air pollution preserved in four Alpine ice cores from 1750 to 2015.
- The increased black carbon emissions in the Southern hemisphere following the extent of human settlements, combining low-latitude lake sediments and Antarctic ice core records.
- Changes of ammonia and nitrogen oxide emissions in South-Eastern Europe inferred from an Elbrus (Caucasus, Russia) ice core record (1774-2009 CE).

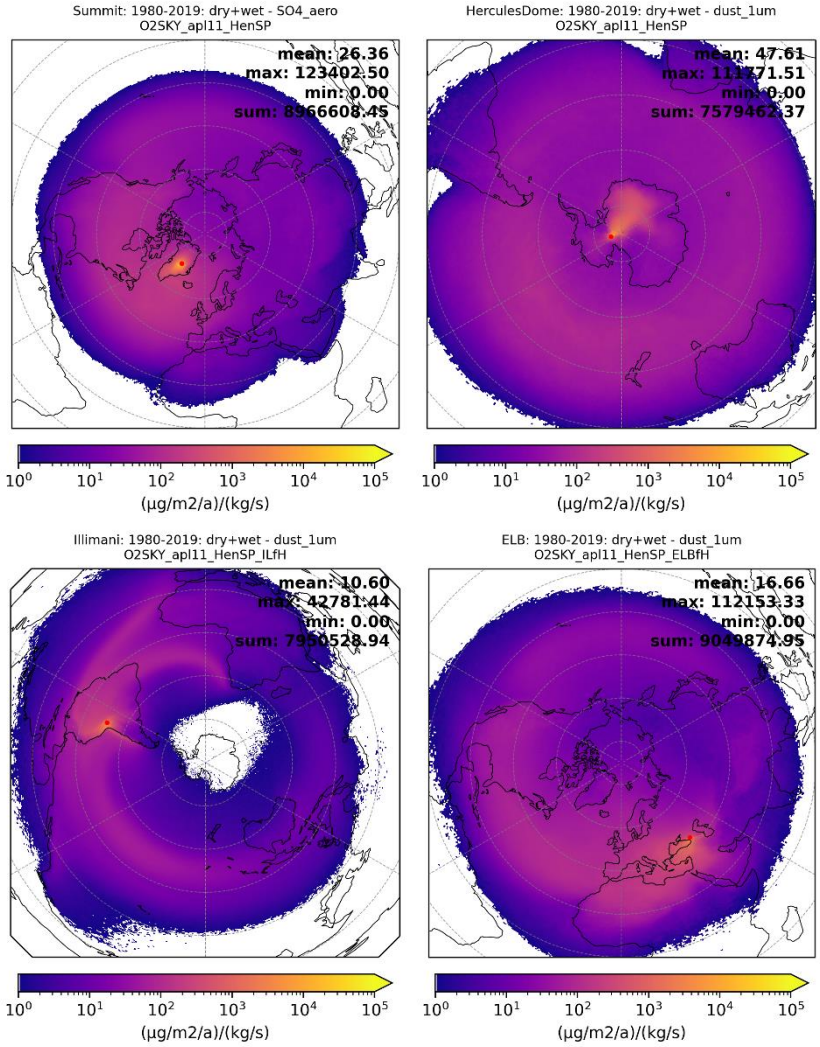

Figure 3: Emission sensitivities for (upper left) the Summit site in Greenland, (upper right) the Hercules Dome site in Antarctica, (lower left) the Illimani site in the Andes, and (lower right) Mt. Elbrus. The respective sites are illustrated by red dots. All plots represent annual mean sensitivities for the period 1980 to 2019; simulated with FLEXPART v10.4 and ERA5 0.5° input data.

4) Moisture sources for the MOSAIC expedition

The Multidisciplinary drifting Observatory for the Study of Arctic Climate (MOSAiC) expedition was a one-year-long expedition into the Arctic (October 2019 to September 2020) with the aim to characterize all aspects of the Arctic atmospheric system from multiple perspectives and across multiple scales (Shupe et al., 2022). The expedition took place on the research vessel Polarstern, which drifted passively in the sea ice during most of the campaign. Aboard Polarstern many meteorological and oceanographic variables were measured, including stable water isotopes in water vapor. Stable water isotopes experience fractionation during phase changes and are therefore useful tracers of Earth's water cycle (Galewsky et al., 2016). Their relative concentration represents the integrated condensation and evaporation history of air parcels and is sensitive to microphysical processes, atmospheric circulation, and moisture source conditions.

To help interpret the stable water isotope measurements during MOSAIC we performed simulations with FLEXPART based on meteorological input data from the ERA5 reanalysis dataset. Every 3 hours we released 100'000 particles from the location of Polarstern and traced them 30 days backward in time. Along the trajectories of the particles we identified moisture uptake regions with the help of the moisture source diagnostic WaterSip (Sodemann et al., 2008). Figure 4 shows the moisture sources for the four seasons of the MOSAIC expedition. Most moisture comes from sea-ice free regions in the Arctic ocean, and the moisture uptakes are higher and more widespread in summer (JJA) and fall (SON) than in winter (DJF) and spring (MAM). Linking the stable water isotope variability with the different moisture sources will help to identify important processes driving the isotope signal at Polarstern and ultimately lead to a better understanding of the Arctic water cycle.

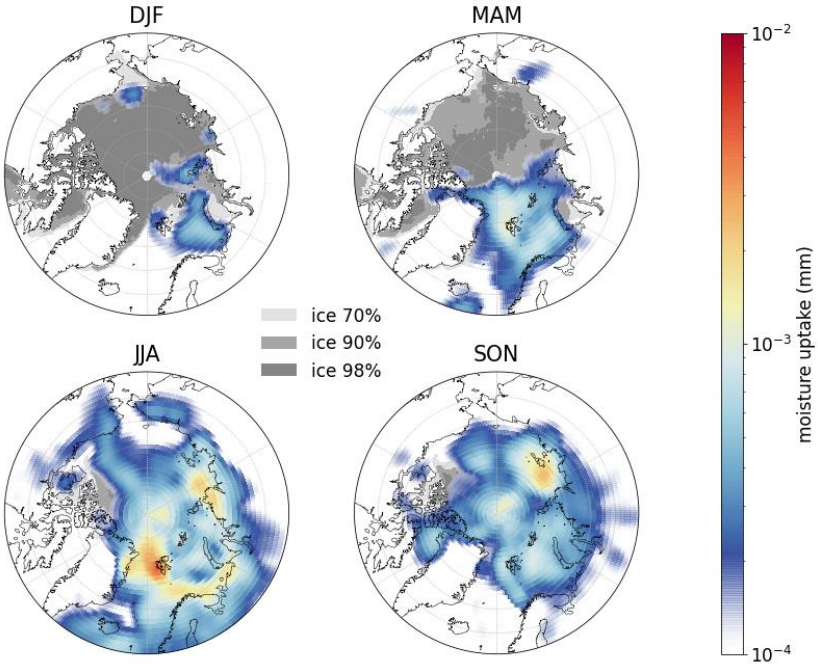

Figure 4: Moisture uptakes in the boundary layer diagnosed by WaterSip for the four seasons of the MOSAIC expedition. Colored shading represents the moisture uptakes, gray shading represents the sea ice concentration.

5) Investigation of the shape effect on atmospheric particles transport

Airborne microplastic particles may have large impacts on human health and, where deposited, on the environment. Therefore, it is crucial to gain more knowledge about transport and removal mechanisms to investigate their in-situ distribution, including transport to remote regions. Most of the atmospheric transport models consider a particle as a perfect sphere, while non-spherical particles experience a larger drag in the atmosphere, which leads to a reduction of their settling velocity and thus longer atmospheric residence times. Hence, model output and ground-based measurements can differ significantly. Currently, we investigate the gravitational settling of the microplastic fibers, the dominant microplastic shape (Rebelein *et al*., 2021). This will help to improve the atmospheric transport models, eliminating uncertainties regarding the shape of a particle, leading to more accurate model simulations of atmospheric concentrations and deposition patterns.

We have implemented shape correction factor developed by Bagheri and Bonadonna, 2016 in the gravitational settling scheme of the Lagrangian transport model FLEXPART v10.4 (Pisso et al., 2019). For FLEXPART simulations in this study, ERA5 reanalysis data is being used. To determine model sensitivity to the shape correction, average atmospheric transport distances and residence times for particles of different sizes and shapes were calculated for assumed particle emissions in different climatic regions and at different release heights. Statistical comparisons of 3D fields of particle mass concentration, dry and wet deposition of implemented and default parameterization schemes will be made. At the moment, a few FLEXPART sensitivity tests have been done. Figure 5 represents the mean mass concentration fields over 30 days of a simulation run in forward mode. The fields correspond to releases of spherical particles and fibers (or cylinders) of the same volume with aspect ratios of 20, 50, and 100.

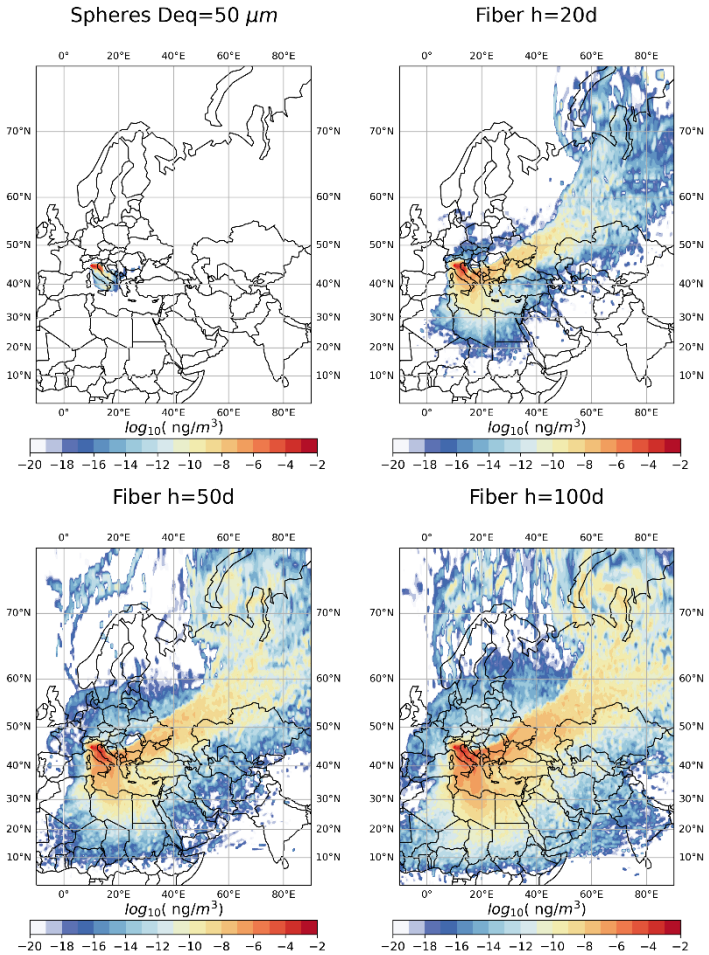

Figure 5: Mean mass concentration fields of particles of different shapes of same volume. Spheres (upper left); cylinders with aspect ratio of: 20 (upper right), 50 (lower left), and 100 (lower right).

6) Sources of NO_y enhancement in the high troposphere during the ATom mission

The Atmospheric Tomography Mission (ATom) has been based on a systematic, global-scale NASA DC-8 aircraft sampling of the atmosphere, profiling continuously from 0.2 to 12 km altitude around the world, with the scope to understand the impact of human-produced air pollution on GHGs and on chemically reactive gases in the atmosphere. Flights were carried out in each of 4 seasons over a 4-year period: ATom-1 (Jul-Aug 2016), ATom-2 (Jan-Feb 2017), ATom-3 (Sep-Oct 2017), and ATom-4 (Apr-May 2018).

During one of the flights (23 October 2017), sampling the atmosphere over USA, the instruments observed an elevated NO and NO_y signal at around 12 km of altitude, in correspondence of a detected cloud presence. NO refers to nitrogen monoxide, the main form in which nitrogen oxides are usually emitted into the atmosphere. Under daylight conditions, by oxidation of ozone and photolysis, a photostationary state between NO and NO_2 is reached within a few minutes, and the sum of these two nitrogen oxides is referred to as NO_x. Within hours to days, NO_x is oxidized into other reactive nitrogen compounds (Bradshaw et al., 2000), the sum of which is referred to as NO_y.

The main sources of NO_y in the atmosphere are lightning, ground emissions and aircraft emissions. In this work we aimed at detecting the relative influence of each of those sources for the 23 October 2017 flight. We performed FLEXPART backward trajectories along the whole flight, releasing a cluster of 100.000 trajectories every 30 minutes along the flight path, travelling back for 7 days. The trajectories computation has been fed with ERA5 data at 0.5 degrees of resolution. The trajectories simulations have been then coupled with proxies of lightning emissions (lightning intensity data from the Geostationary Lightning Mapper (GLM, https://ghrc.nsstc.nasa.gov/lightning/overview_glm.html), aviation emissions (aircrafts tracks, from flightradar24, https://www.flightradar24.com/) and ground emissions (from the ECLIPSE v5 database, https://previous.iiasa.ac.at/web/home/research/researchPrograms/air/ECLIPSEv5.html).

Each relative contribution has been then compared and weighted, by multiple regression analysis methods, to the NO_y observations. The results are illustrated in Figure 6. While the aviation contribution is the dominant one along the whole flight with an average enhancement of around 0.13 ppbv, the strongest enhancement of NO_y is due to the encounter of lighting events (time of transport of few hours, estimated from the FLEXPART analysis), which cause a concentration increase up to 1.4 ppbv in a layer between 10 and 12 km of altitude. The ground contribution from anthropogenic activities instead does not appear to significantly affect the concentration in the regions investigated by the aircraft (average contribution 0.05 of ppbv). The role of a fresh contribution from lightning is also confirmed by the corresponding enhancement of NO, which corresponds to the biggest fraction of NO_y.

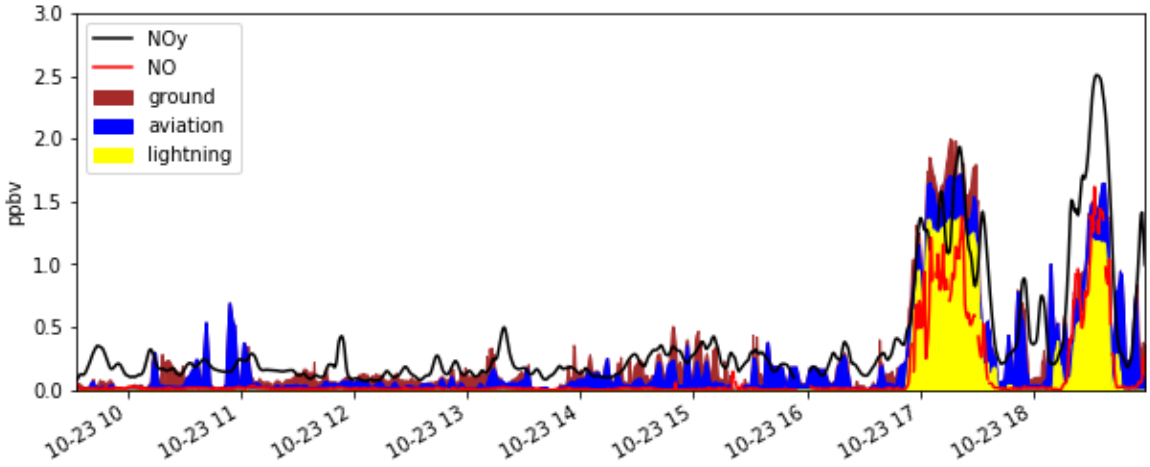

Figure 6: NO_y source contributions simulated with FLEXPART v10.4 fed by ERA5 0.5° data. The coloured layers indicate the simulated relative contribution of each source (ground anthropogenic emission, aviation and lightning) in ppbv. The solid black and red lines indicate the observed NO_y and NO concentration, respectively.

Summary of plans for the continuation of the project (10 lines max)

Following our findings, we will apply the GDB method and longer backward simulation periods (such as 50 days) preforming inverse modelling to a range of different GHGs to investigate their flux changes over the last one or two decades. We will continue analysing the emission sensitivity of ice core sites. Furthermore, we plan to use FLEXPART to analyse the sensitivity of a Swiss tall tower site measuring GHGs and further constrain Swiss GHG emission source regions. Additionally, deposition data of microplastics, collected in remote regions of Siberia, Russia, will be used to evaluate model predictions by using backward simulations. Moreover, the aforementioned 3D fields of microplastics will be simulated by estimating their emissions according to the global population density. This will help to estimate the contribution of the individual regions to microplastic contamination of the atmosphere, land, and World Ocean.

List of publications/reports from the project with complete references

Vojta, M., Plach, A., Thompson, R. L., and Stohl, A.: 'A comprehensive evaluation of the use of Lagrangian particle dispersion models for inverse modeling of greenhouse gas emissions', EGUsphere [preprint], https://doi.org/10.5194/egusphere-2022-275, 2022.

References:

Bagheri, G. and Bonadonna C. (2016) 'On the drag of freely falling non-spherical particles', Powder Technology, 301, pp. 526–544., https://doi.org/10.1016/j.powtec.2016.06.015

Bradshaw, J., Davis, D., Grodzinsky, G., Smyth, S., Newell, R., Sandholm, S., & Liu, S. (2000). Observed distributions of nitrogen oxides in the remote free troposphere from the NASA global tropospheric experiment programs. Reviews of Geophysics, 38(1), 61-116., https://doi.org/10.1029/1999RG900015

Galewsky, J., Steen-Larsen, H. C., Field, R. D., Worden, J., Risi, C., & Schneider, M. (2016). Stable isotopes in atmospheric water vapor and applications to the hydrologic cycle. Reviews of Geophysics, 54(4), 809-865, https://doi.org/10.1002/2015RG000512

Pisso, I., Sollum, E., Grythe, H., Kristiansen, N. I., Cassiani, M., Eckhardt, S., Arnold, D., Morton, D., Thompson, R. L., Groot Zwaaftink, C. D., Evangeliou, N., Sodemann, H., Haimberger, L., Henne, S., Brunner, D., Burkhart, J. F., Fouilloux, A., Brioude, J., Philipp, A., Seibert, P., and Stohl, A.: (2019) 'The Lagrangian particle dispersion model FLEXPART version 10.4', Geoscientific Model Development, 12(12), pp. 4955–4997., https://doi.org/10.5194/gmd-12-4955-2019.

Rebelein A., I. Int-Veen, U. Kammann, J.P. Scharsack, (2021) 'Microplastic fibers - underestimated threat to aquatic organisms?', Science of a Total Environment, 777, p. 146045., https://doi.org/10.1016/j.scitotenv.2021.146045

Ruckstuhl, A. F., Henne, S., Reimann, S., Steinbacher, M., Vollmer, M. K., O'Doherty, S., Buchmann, B., and Hueglin, C. (2012) 'Robust extraction of baseline signal of atmospheric trace species using local regression', Atmospheric Measurement Techniques, 5(11), pp. 2613–2624., https://doi.org/10.5194/amt-5-2613-2012.

Shupe, M. D., Rex, M., Blomquist, B., Persson, P. O. G., Schmale, J., Uttal, T., ... & Yue, F. (2022). Overview of the MOSAiC expedition: Atmosphere. Elem Sci Anth, 10(1), 00060., https://doi.org/10.1525/elementa.2021.00060

Sodemann, H., Schwierz, C., & Wernli, H. (2008). Interannual variability of Greenland winter precipitation sources: Lagrangian moisture diagnostic and North Atlantic Oscillation influence. Journal of Geophysical Research: Atmospheres, 113(D3)., https://doi.org//10.1029/2007JD008503

Stohl, A., Forster, C., Frank, A., Seibert, P., and Wotawa, G.: Technical note: (2005) 'Technical note: The Lagrangian particle dispersion model FLEXPART version 6.2', At-mospheric Chemistry and Physics. Copernicus GmbH, 5(9), pp. 2461–2474., https://doi.org/10.-5194/acp-5-2461-2005.

Stohl, A., Seibert, P., Arduini, J., Eckhardt, S., Fraser, P., Greally, B. R., Lunder, C., Maione, M., Mühle, J., O'Doherty, S., Prinn, R. G., Reimann, S., Saito, T., Schmidbauer, N., Simmonds, P. G., Vollmer, M. K.,Weiss, R. F., and Yokouchi, Y.: (2009) 'An analytical inversion method for determining regional and global emissions of green-house gases: Sensitivity studies and application to halocarbons', Atmospheric Chemistry and Physics. Coper-nicus GmbH, 9(5), pp. 1597–1620., https://doi.org/10.5194/acp-9-1597-2009.